JECS 1572c

0955-2219(95)00081-X

Journal of the European Ceramic Society **16** (1996) 63–70
Elsevier Science Limited
Printed in Great Britain.
0955-2219/96/$15.00

Modification of PTCR Behavior of $(Sr_{0.2}Ba_{0.8})TiO_3$ Materials by Post-Heat Treatment after Microwave Sintering

Horng-Yi Chang,[a] Kuo-Shung Liu[a] & I.-Nan Lin[b]

[a]Department of Materials Science and Engineering, and [b]Materials Science Center, National Tsing-Hua University, Hsinchu, 30043 Taiwan, Republic of China

(Received 13 February 1995; revised 18 May 1995; accepted 19 May 1995)

Abstract

$(Sr_{0.2}Ba_{0.8})TiO_3$ materials have been effectively densified by microwave sintering process. The grain size (~ 6 μm) and PTCR characteristics (T_c = 50°C, $\rho_{max}/\rho_{min} \approx 10^2$) of the as-sintered samples vary insignificantly with sintering temperature (1100–1180°C) and soaking time (10–40 min). However, lowering the cooling rate after sintering substantially increases the resistivity jump (ρ_{max}/ρ_{min}) from 10^2 to $10^{5.3}$, without altering the microstructure. Subsequent annealing, on the other hand, substantially modifies the microstructure and PTCR characteristics. The resistivity jump increases monotonously with heat treatment temperature (T_{ht}) and reaches (ρ_{max}/ρ_{min}) $\approx 10^7$ for samples heat-treated at 1300°C for 2 h. The grain size remains nearly unchanged for $T_{ht} \leq 1200$°C and grows markedly for samples heat-treated at a higher temperature. The effective trap level is estimated to be E_s = 1·46 eV. The activation energy for the densification rate is Q_{MS} = 8·2 kcal/mol for microwave sintering and Q_{cs} = 62·5 kcal/mol for conventional sintering process.

1 Introduction

Since their discovery in 1955, semiconducting $BaTiO_3$ materials, which possess positive temperature coefficient of resistivity (PTCR) characteristics, have found extensive application as thermistors, safety circuits, degaussers, and other devices.[1,2] The models of Heywang and Jonker[3–5] are the most popular conduction models used to account for the PTCR behavior of these materials. According to these models, the Schottky barrier induced by the surface states existing at grain boundary regions leads to high resistivity of the materials in the paraelectric phase at a temperature higher than the Curie temperature (T_c). The spontaneous polarization which occurs in the ferroelectric state, when $T < T_c$, results in compensation of surface states[5,6] and lowers the resistivity of the materials. Therefore, the concentration of effective surface states, N_s, is one of the dominating factors which determine the resistivity jump of the materials. The PTCR characteristics of these materials are, thereby, tremendously influenced by the processing parameters which modify the surface states of the materials.[7–15]

The preparation of these materials by conventional sintering process normally requires a very high sintering temperature (>1350°C), even when liquid phase sintering aids are applied[16]. The microwave sintering process, on the other hand, has been observed to densify the ceramic materials at a very rapid rate and at a substantially lower temperature.[17–21] This technique is, therefore, adopted in this study in an attempt to rapidly sinter the donor-doped $(Sr_{0.2}Ba_{0.8})TiO_3$ materials. The effect of processing parameters, such as sintering temperature, soaking time, cooling rate and the post-heat treatment schemes, on the microstructure and PTCR properties of these materials is systematically examined. The correlation of the defect chemistry possibly occurred during processing with the electrical behavior of the samples will be discussed.

2 Experimental Procedure

The $(Sr_{0.2}Ba_{0.8})TiO_3$ powders, which contained 0·3 mol% Sb_2O_3 as semiconductive dopants and 5 mol% AST (Al_2O_3:SiO_2:TiO_2 = 4:9:3) as sintering aids, were prepared by the conventional mixed oxide method. In which, the mixtures containing high purity oxides of proper proportion were ball-milled in a plastic jar, using plastic-coated iron

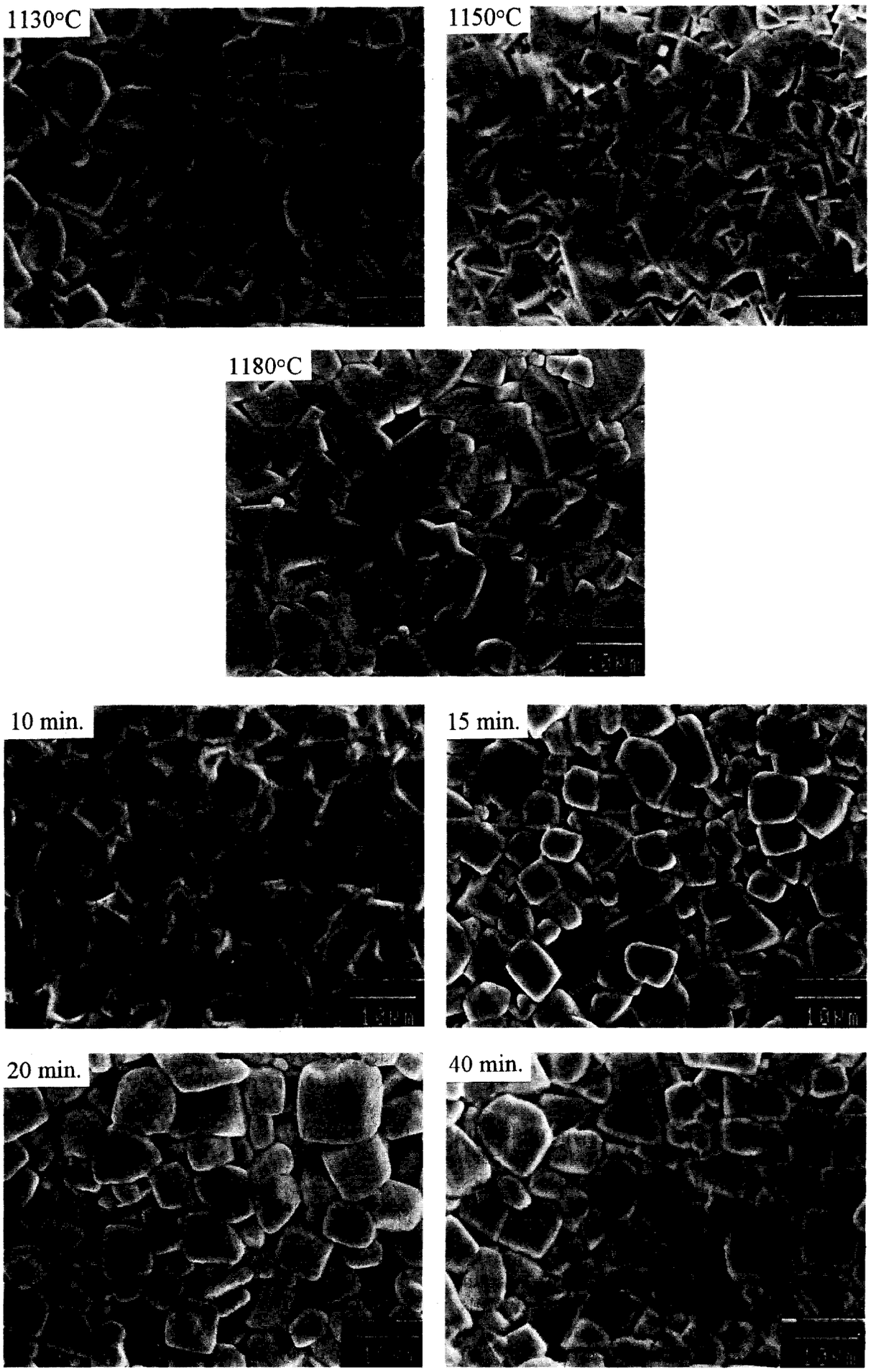

Fig. 1. Microstructure of the $(Sr_{0.2}Ba_{0.8})TiO_3$ samples microwave sintered: (a) at 1130–1180°C for 40 min and (b) at 1130°C for 10–40 min, cooled at 154°C/min.

balls, with deionized water, for 8 h. They were then calcined at 1000°C in air for 4 h, followed by pulverization in a ball-mill for 8 h to around 1 μm size. The green compacts made of these powders were heated at 600°C for 1 h to remove the binders (PVA) and then microwave sintered at 1100–1180°C for 10–40 min in an applicator made of WR284 waveguide. The 2·45 GHz microwave generated from commercial source (Gerling GL107 magnetron) was used to heat up the samples. The temperature profile was then measured using Pt–13%Rh thermocouple, placed near the sample surface. The heating rate was controlled at 50°C/min and the cooling rate was varied (4°C/min, 9°C/min, or 154°C/min). In the annealing experiments, the materials microwave sintered at 1130°C for 40 min (cooled at 154°C/min) were heat-treated at either 1000, 1130, 1200, 1250, or 1300°C for 2 h in an electrical furnace. The heating and cooling rate in the annealing process were all controlled at 5°C/min. To facilitate the comparison of the microwave sintering process with the conventional sintering process, the green compacts of the same materials were sintered in a resistive heating furnace by a two-step process. The samples were preheated at 1200°C for 2 h, followed by rapidly heating to 1225, 1250, 1275 or 1300°C and then sintered at that temperature for 2 h. The preheating and cooling rate were controlled at 5°C/min.

The density of the samples is measured by Archimedes' method and the densification rate is calculated by dividing the change in density value by the time interval at temperature. The crystal structure and microstructure of the sintered samples were examined using Rigaku D/max-IIB X-ray diffractometer and Joel JSM-840A scanning electron microscope (SEM), respectively. The average grain size of the samples is estimated from the SEM micrographs by linear interception method. The resistivity–temperature (ρ–T) properties of these samples were measured using H.P. 3457A multimeter after the In–Ga alloy was rubbed onto the sample surface to serve as electrodes.

3 Results

The beneficial effect of microwave sintering technique on enhancing densification process of the $(Sr_{0.2}Ba_{0.8})TiO_3$ material is enormous, as illustrated by the fact that the samples microwave-sintered at 1180°C for 20 min already reach the same density (~ 95% T.D.) as those sintered by the furnace-heating process at 1300°C for 2 h. In other words, the diffusivity of the cations and anions in these materials is substantially enhanced in the microwave sintering process. The microstructure of the samples varies insignificantly with the sintering temperature and soaking time. The grain size of the samples increases slightly with sintering temperature, from around 6 μm for 1130°C-sintered samples to around 9 μm for 1180°C-sintered samples (Fig.1(a)) and the grain size is around 6μm for all samples microwave sintered at 1130°C for 10–40 min (Fig. 1(b)).

To facilitate the comparison, the microstructures of the $(Sr_{0.2}Ba_{0.8})TiO_3$ materials sintered by conventional method in two-step process are shown in Figs 2(a)–(c). These figures indicate that the growth of the grains can be triggered only when the sintering temperature is higher than 1275°C, which is slightly higher than the eutectic point reported[16] for $(Sr_{0.2}Ba_{0.8})TiO_3$ and AST system. Compared to the microstructure of the samples directly sintered at 1300°C for 2 h shown in Fig. 2(d), the uniformity of the grain size distribution has been substantially improved by a two-step sintering process, and that of the microwave sintered samples is even better (c.f. Fig.1). The temperature range suitable for the microwave sintering process is, however, very narrow. The materials are hardly sintered when the sintering temperature is maintained at 1100°C or lower. The sintering process is rather unstable and the thermal runaway phenomenon frequently occurs when the sintering temperature is increased to 1190°C or higher. The crystal structure of the calcined powders and the as-microwave sintered $(Sr_{0.2}Ba_{0.8})TiO_3$ samples are shown in Figs 3(a) and (b), respectively. The (002) and (200) diffraction peaks are only barely split, indicating that the c/a ratio of the materials is very small. The tetragonality, (i.e. c/a ratio) of the samples does not vary with the temperature and soaking time in the microwave sintering process. It is also not significantly different from that of the conventionally-sintered samples (c.f. Fig. 3(d)).

To further elucidate how the microwave sintering process enhances the sintering behavior of the (Sr, Ba)TiO_3 materials, the activation energy (Q) for the densification process is evaluated from the densification rate of the samples. For this purpose, a simplified densification theory[23] was adopted, that is,

$$dg/dt = \mathrm{JAN}\Omega = (96\pi\gamma\Omega/kTG^3)\cdot D_0\exp(-Q/kT) = (K/T)\cdot D_0\exp(-Q/kT)$$

where J is the diffusive flux, A is the area over which diffusion acts, N is number density of pores and Ω is the atomic volume. Moreover, γ is surface energy, G is grain size and K is a geometric factor, D_0 is the pre-exponential term of diffusivity, k and T are the Boltzmann constant and temperature, respectively, and dg/dt is the densification

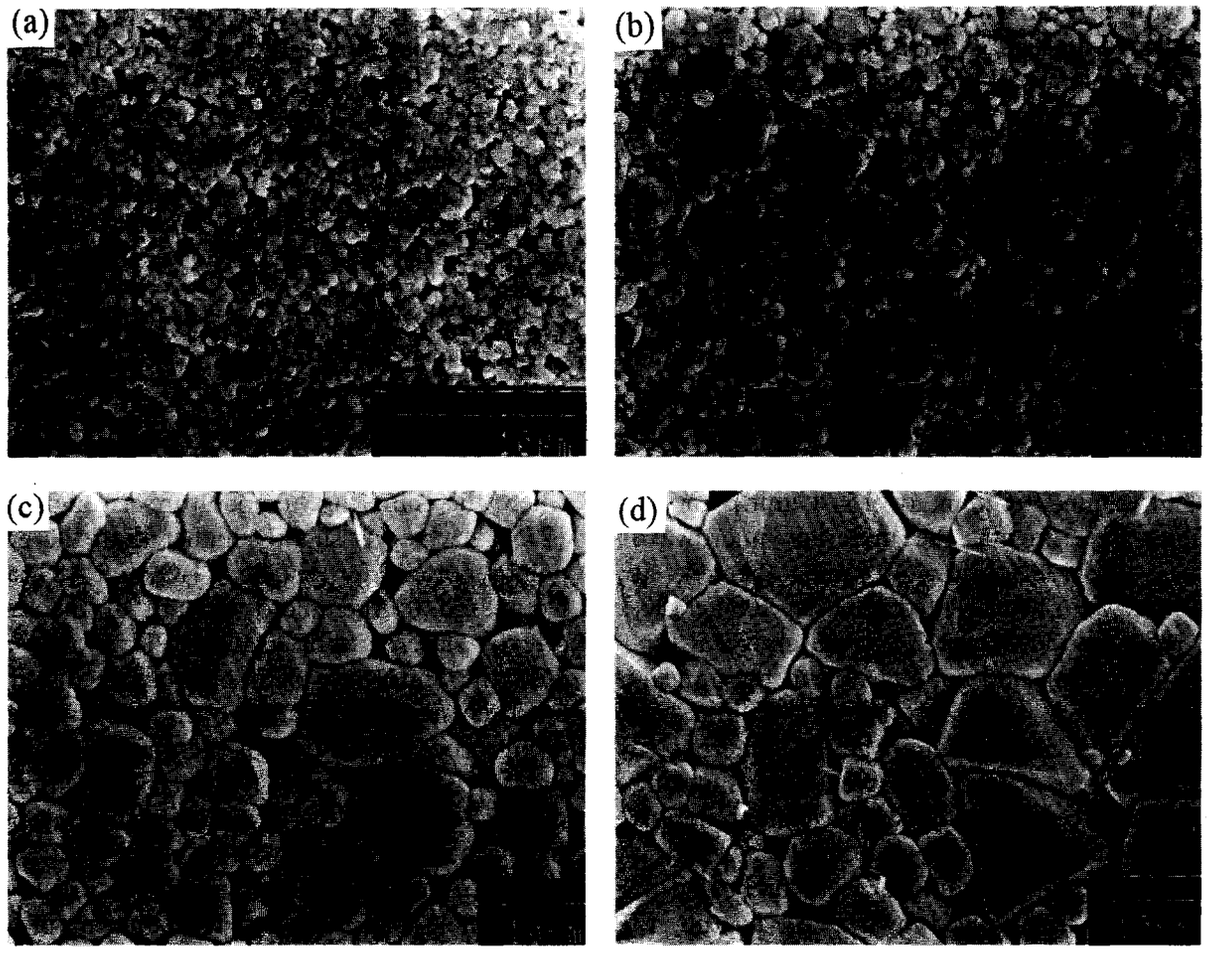

Fig. 2. The microstructure of $(Sr_{0.2}Ba_{0.8})TiO_3$ samples sintered by conventional method in two-step process: (a) 1200°C-2 h; (b) 1275°C-2 h after 1200°C-2 h; (c) 1300°C-2 h after 1200°C-2 h and (d) that directly sintered at 1300°C-2 h.

rate of the samples. The activation energy (Q) for densification can be estimated from the Arrhenius plot of the densification rate. Figure 4, in which the density of the microwave-sintered and furnace-sintered samples are listed as the inset, shows that the activation energy for densification in microwave sintering process (Q_{MS} = 8·2 kcal/mol) is significantly smaller than that of the conventional sintering process (Q_{cs} = 62·5 kcal/mol). The deviation of the data corresponding to the samples furnace-sintered at 1275 or 1300°C (open triangles) from the Arrhenius plot is presumably caused by the change in the densification mechanism, since the liquid phase is expected to occur for these samples at these temperatures. The samples are densified by solid state diffusion mechanism when sintering temperature is lower.

The above mentioned results indicate that the microwave sintering process can densify the $(Sr_{0.2}Ba_{0.8})TiO_3$ materials at a substantially lower temperature than the conventional sintering process.

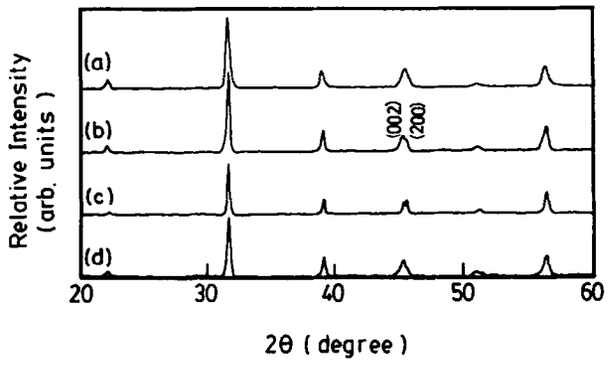

Fig. 3. The X-ray diffraction patterns of $(Sr_{0.2}Ba_{0.8})TiO_3$ samples: (a) as calcined powders; (b) as microwave sintered (at 1180°C for 40 min); (c) 1200°C-2 h annealed (after microwave sintering) and (d) the 1300°C-2 h conventionally sintered samples.

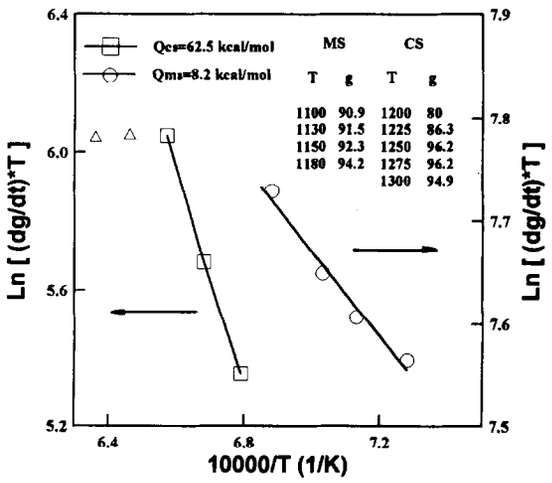

Fig. 4. The Arrhenius plots for densification rate of the samples sintered by the microwave sintering process (MS) and the conventional sintering process (CS). The inset shows the density of these samples. (T: sintering temperature in °C; g: density in % of theoretical density).

The additional benefit of utilizing the microwave sintering technique is the capability of initiating the densification process without triggering the grain boundary migration. Consequently, the materials are densified without grain growth, leading to a microstructure with a fine and very uniform grain size distribution. The microwave sintering process is, therefore, substantially advantageous over the conventional sintering process in the preparation of the $(Sr_{0.2}Ba_{0.8})TiO_3$ PTCR materials.

The resistivity–temperature properties of the samples vary moderately with the sintering temperature and soaking time. The minimum (ρ_{min}) and maximum (ρ_{max}) resistivity of the samples alter only slightly with the sintering conditions. The resistivity ratio ($\alpha = \rho_{max}/\rho_{min}$) slightly increases with sintering temperature but varies insignificantly with soaking time (Fig. 5, curve 3). The positive temperature coefficient of resistivity (PTCR) of these samples, which is defined as

$$p = \{(\log\rho_{-Tc+\Delta T} - \log\rho_{Tc})/\Delta T\}$$

is around $p = 0{\cdot}01$ Ω·cm/°C for $T_c = 50$°C and $\Delta T = 100$°C, and the resistivity ratio is around $\alpha = 10^{1{\cdot}75}$. The Curie temperature of these samples is roughly the same ($T_c \approx 50$°C).

According to the Heywang and Jonker[3–5] models, the PTCR behavior of these materials primarily arises from the Schottky barrier formed at grain boundary regions. Besides the common practices to modify the potential barrier by artificially doping some modifiers, (e.g. Mn),[9–10] the cooling rate after sintering has been observed to effectively modify the defect chemistry near the grain boundary regions by the oxidation–reduction process so as to increase the PTCR behavior of $BaTiO_3$[11] and (Sr, Ba)TiO_3[12] samples. The same approach is thereby adopted here to improve the PTCR properties of the microwave sintered samples. Figure 5 shows that reducing the cooling rate does lead to

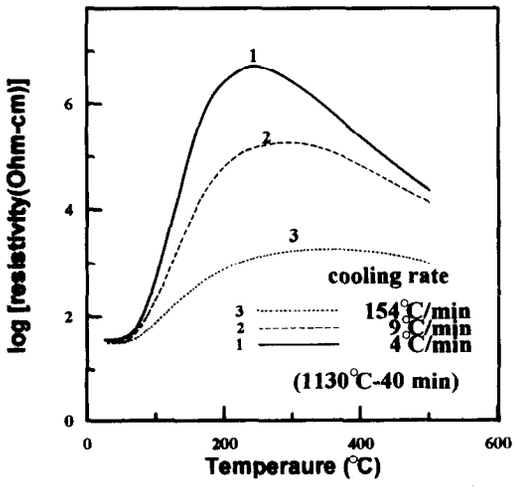

Fig. 5. The resistivity–temperature properties of the $(Sr_{0.2}Ba_{0.8})TiO_3$ samples as microwave sintered at 1130°C (40 min) and cooled at different rate (4–154°C/min).

a tremendous change in resistivity–temperature characteristics. It does not cause any significant modification on the microstructure of the samples. As the cooling rate decreases, the maximum resistivity (ρ_{max}) increases markedly while the minimum resistivity (ρ_{max}) remains unchanged, such that the resistivity jump ($\alpha = \rho_{max}/\rho_{min}$) increases substantially from $\alpha = 10^{1{\cdot}75}$ ($p = 0{\cdot}01$ Ω·cm/°C) for 154°C/min-cooled samples to $\alpha = 10^{4{\cdot}85}$ ($p = 0{\cdot}04$ Ω·cm/°C) for 4°C/min-cooled samples. The temperature of maximum resistivity (T_{max}) shifts slightly towards a lower temperature as the cooling rate after sintering is reduced. Similar behavior has also been observed in the $BaTiO_3$ and $(Sr_{0.2}Ba_{0.8})TiO_3$ materials sintered by conventional process[11,12] and was accounted for by the model that the grain boundary regions are richer in cationic vacancies, due to the compensation of the oxygen vacancies by the inward diffused oxygen ions during the cooling period. These atomic vacancies act as effective electron traps and increase the Schottky barrier height of the materials. This model is adopted to quantitatively estimate the effective trap level induced in Fig. 5 and will be discussed later.

The residue stress induced by the isostatic pressure is another factor which has been reported to markedly influence the dielectric constant and, hence, the Schottky barrier height of the (Sr, Ba)TiO_3[24] materials. The 1130°C (40 min) sintered (154°C/min cooled) samples were thus heat-treated at 1000–1200°C for 2 h and then slowly cooled (5°C/min) to examine the influences of residual stress possibly induced by a rapid cooling process on the characteristics of these materials. Figures 6(a–c) show that the microstructure of these samples has not been modified. The contrasting increase of the grain boundaries in the micrograph of 1200°C-annealed samples (Fig. 6(c)) is due to the thermal etching effect on the polished samples. On the other hand, Fig. 7(a) indicates that the maximum resistivity (ρ_{max}) of the samples was increased and the T_{max}-value was also shifted towards a lower temperature for the samples heat-treated. The higher the heat treatment temperature the larger the modification is.

The other phenomenon of interest is the influence of grain size on the PTCR properties of the materials. Figures 6(c–e) illustrate that the grains start to grow when the heat treating temperature (T_{ht}) is higher than 1250°C. The variation of grain size with T_{ht} is plotted in the inset of Fig. 7. The X-ray diffraction patterns shown in Fig. 3(c) infer that the tetragonality of the materials remains the same. The ρ–T curves in Fig. 7(b) show that the ρ_{max} value abruptly increases and the resistivity ratio markedly jumps whenever the grain growth has occurred. Excellent PTCR behavior is obtained

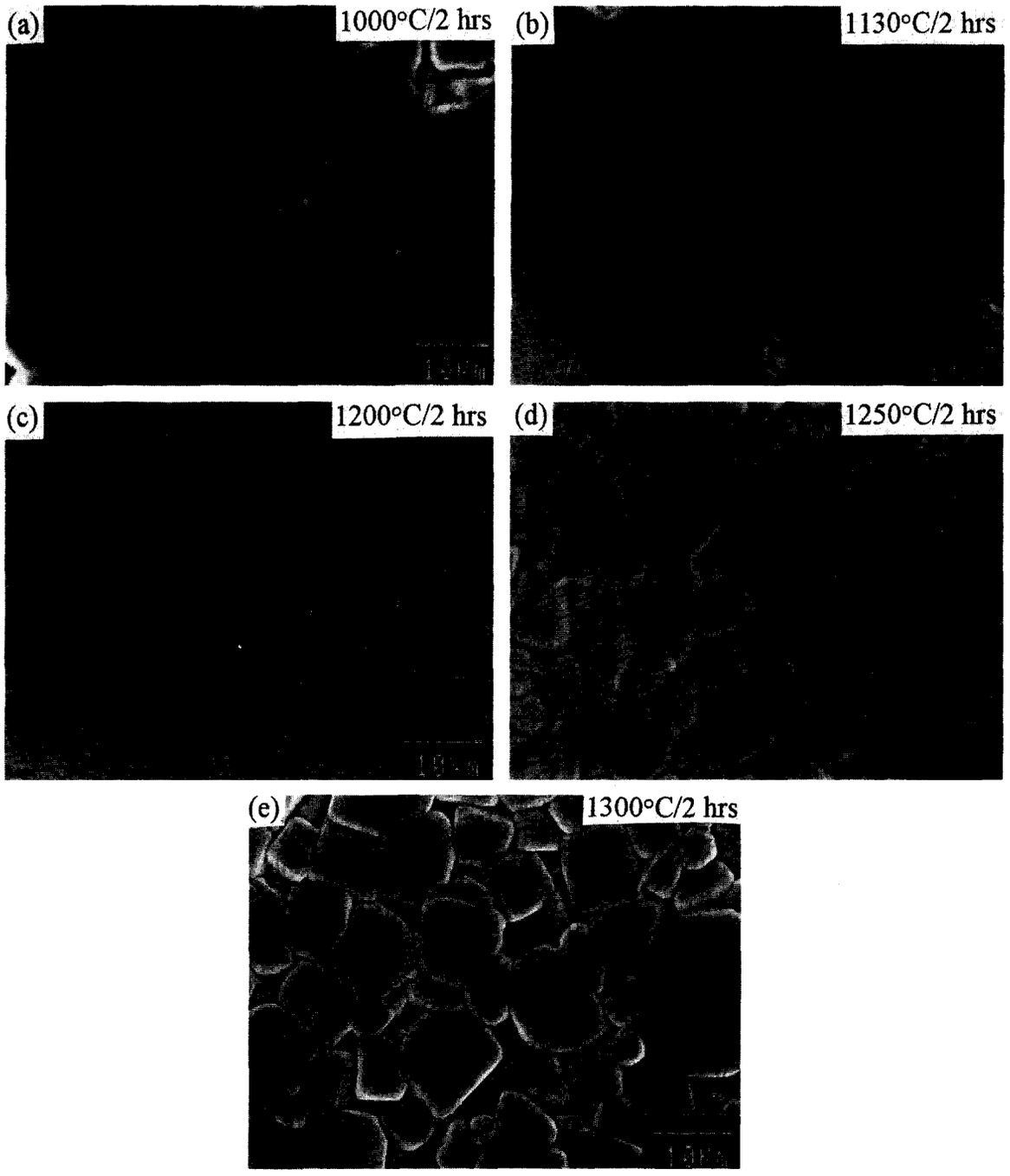

Fig. 6. The microstructure of $(Sr_{0.2}Ba_{0.8})TiO_3$ samples microwave sintered at 1130°C for 40 min and heat treated at: (a) 1000°C; (b) 1130°C; (c) 1200°C; (d) 1250°C and (e) 1300°C for 2 h.

for samples heat-treated at 1300°C for 2 h ($\alpha = 10^7$, $p = 0{\cdot}053\ \Omega$·cm/°C). Interestingly; the grain size of the 1300°C (2 h) heat-treated samples (microwave-sintered) is the same as that of the samples sintered by a conventional method, (two-step process) at 1300°C for 2 h (c.f Figs 2(c) and 6(e)). The tetragonality of the two samples are almost the same (c.f. Figs 3(c) and (d)). However, the ρ–T characteristics of the microwave-sintered samples (after heat treatment), which is shown as a dash–dotted curve in Fig. 7(b), are significantly superior to that of the conventionally sintered samples (dotted curve, Fig. 7(b)). This phenomenon reveals the importance of having a uniform grain size distribution on the electrical properties of the PTCR materials.

4 Discussion

The annealing process after microwave sintering was observed to modify the PTCR behavior of the $(Sr_{0.2}Ba_{0.8})TiO_3$ material in a very similar way with the cooling rate did, *viz.*, the T_{max}-value lowered as the ρ_{max} increased (c.f. Figs. 5 and 7). The increase in resistivity, accompanied by the decrease in T_{max}-value, due to slow cooling rate has been ascribed to the increase in the concentration of the effective electron traps, i.e. cationic vacancies.[11,12] The same mechanism is adopted to account for the effect of heat treatment on the ρ–T behavior shown in Fig. 7. In other words, the cationic vacancies, which act as effective electron

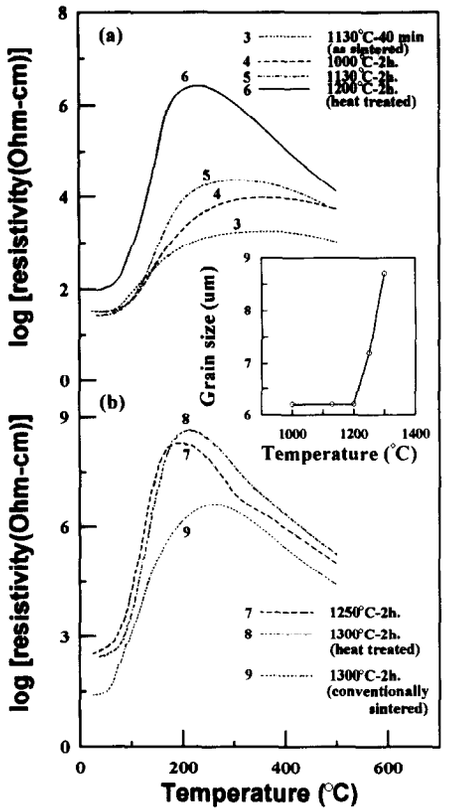

Fig. 7. The resistivity–temperature (ρ–T) properties of $(Sr_{0.2}Ba_{0.8})TiO_3$ samples microwave sintered at 1130°C and then heat treated (a) at 1000–1200°C for 2 h, including that of the as-sintered samples (dotted curve) and (b) at 1250–1300°C for 2 h, including that of the samples sintered by conventional process at 1300°C for 2 h (dotted curve). The inset shows the grain size of the annealed samples.

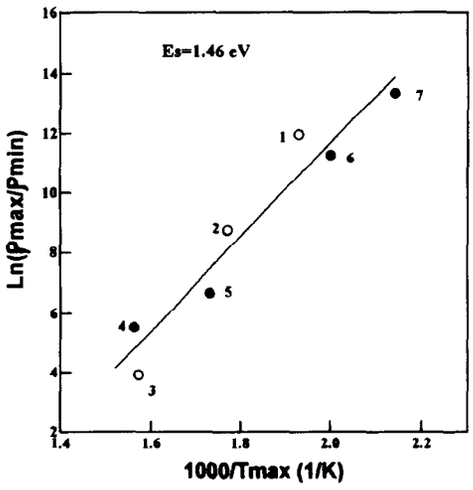

Fig. 8. The $\log(\rho_{max}/\rho_{min})$–$T_{max}^{-1}$ plot of the resistivity–temperature curves for estimating the effective trap level; open symbols and closed symbols correspond to the ρ–T curves in Figs 5 and 7, respectively.

traps, are larger in concentration when heat-treated at higher temperature. This occurs probably due to the fact that the equilibrium concentration of cationic and anionic vacancy pairs generated at higher temperature is larger so that the residue concentration of the cationic vacancies, after re-oxidation due to inward diffusion of oxygen during cooling process, is significantly higher.

Since the samples shown in Figs 5 and 7 are of similar microstructure and the cooling rate during microwave sintering or post-annealing process only modifies the concentration of effective electron traps, i.e. cationic vacancies, the energy level of these effective traps can be evaluated from the $\log(\rho_{max}/\rho_{min})$–$T_{max}^{-1}$ plot.[11] The (ρ_{max}/ρ_{min}) and T_{max} values estimated from ρ–T curves in Figs 5 and 7 are plotted in Fig. 8, showing that the energy levels of the effective traps (E_s) induced by cooling rate process (open circles) is very close to that by the annealing process (solid circles). That is, E_s = 1·36 eV + *Ef*. This phenomenon confirms again, that the effective electron traps induced in the two processes are of the same nature. The Fermi level (E_f) of the $(Sr_{0.2}Ba_{0.8})TiO_3$ semiconducting oxide is usually close to the donor level ($E_d \approx 0{\cdot}1$ eV)[25] in the donor-doped materials. The effective trap level is, therefore, concluded to be $E_s \approx 1{\cdot}46$ eV.

5 Conclusions

The microwave sintering process has been observed in this study to effectively densify the $(Sr_{0.2}Ba_{0.8})TiO_3$ materials at substantially lower temperature than the conventional sintering process does. However, the sintering temperature should be controlled in a very narrow range (1130–1180°C). Neither the sintering temperature nor the soaking time in the microwave sintering process shows significant influence on the PTCR behavior and the microstructure of the as-microwave sintered samples. Contrarily, the cooling rate at the end of sintering cycle or the post-heat treatment after sintering exhibits a tremendous effect on increasing the PTCR properties of the samples. The resistivity jump (ρ_{max}/ρ_{min}) reaches 10^7 for samples heat-treated at 1300°C for 2 h. The effective trap level is estimated to be around $E_s \approx 1{\cdot}46$ eV and is assumed to have been resulted from the excess cationic vacancies residing in the regions near grain boundaries. The activation energy for the densification in the microwave sintering process is estimated to be Q_{MS} = 8·2 kcal/mol, which is significantly smaller than that of the conventional sintering process (Q_{cs} = 62·5 kcal/mol).

Acknowledgment

The authors would like to thank the National Science Council, Republic of China, for financial support of this manuscript under Contract No. NSC83-0404-E-007-050.

References

1. Wakino, K. & Fujikawa, N., $BaTiO_3$ and its applications. *Electron. Ceram.*, **2**(5) (1971) 73–6.
2. Wakino, K. & Fujikawa, N., Semiconducting $BaTiO_3$ and its applications. *Electron. Ceram.*, **2**(7) (1971) 65–71.
3. Heywang, W., Barium titanate as a semiconductor with blocking layers. *Solid-State Electron.*, **3** (1961) 51–8.
4. Heywang, W., Resistivity anomaly in doped barium titanate. *J. Am. Ceram Soc.*, **47**(10) (1964) 484–90.
5. Jonker, G. H., Some aspects of semiconducting barium titanate. *Solid-State Electron.*, 7 (1964) 895–903.
6. Huybrechts, B., Ishizaki, K. & Takata, M., Experimental evaluation of the acceptor-states compensation in positive-temperature-coefficient-type barium titanate. *J. Am. Ceram. Soc.*, **75**(3) (1992) 722–4.
7. Alles, A. B., Amarakoon, V. R. W. & Burdick, V. L., Positive temperature coefficient of resistivity effect in undoped, atmospherically reduced barium titanate. *J. Am. Ceram. Soc.*, **72**(1) (1989) 148–51.
8. Al-Allak, H. M., Brinkman, A. W., Russell, G. J. & Woods, J., The effect of Mn on the positive temperature coefficient of resistance characteristics of donor doped $BaTiO_3$ ceramics. *J Appl. Phys.*, (1988) 4530–5.
9. Illingsworth, J., Al-Allak, H. M., Brinkman, A. W. & Woods, J., The influence of Mn on the grain-boundary potential barrier characteristics of donor-doped $BaTiO_3$ ceramics. *J. Appl. Phys.*, **67**(4) (1990) 2088–92.
10. Ihrig, H., PTC effect in $BaTiO_3$ as a function of doping with 3d elements. *J. Am. Ceram. Soc.*, **64**(10) (1981) 617–20.
11. Lin, T. F., Hu, C. T. & Lin, I. N., Defects restoration during cooling and annealing in PTC type barium titanate ceramics. *J. Mater. Sci.*, **25** (1990) 3029–33.
12. Chen, H. P. & Tseng, T. Y., The effect of cooling rate on the positive temperature coefficient resistivity characteristics of lanthanum-doped $Ba_{0.8}Sr_{0.2}TiO_3$ ceramics, *J. Mater. Sci. Lett.*, **8** (1989) 1483–5.
13. Huybrechts, B., Ishizaki, K. & Takata, M., Influence of high oxygen partial pressure annealing on the positive temperature coefficient of Mn-doped $Ba_{0.8}Sr_{0.2}TiO_3$ *J. Europ. Ceram. Soc.*, **11** (1993) 395–400.
14. Huybrechts, B., Ishizaki, K. & Takata, M., Proposed phenomenological PTCR model and accompanying phenomenological PTCR chart. *J. Am. Ceram. Soc.*, **77**(1) (1994) 286–8.
15. Al-Allak, H. M., Russell, G. J. & Woods, J., The effect of annealing on the characteristics of semiconducting $BaTiO_3$ positive temperature coefficient of resistance devices. *J. Phys. D: Appl. Phys.*, **20** (1987) 1645–51.
16. Cheng, H. F., Lin, T. F., Hu, C. T. & Lin, I. N., Effect of sintering aids on microstructures and PTCR characteristics of $(Sr_{0.2}Ba_{0.8})TiO_3$ ceramics. *J. Am. Ceram. Soc.*, **76**(4) (1993) 827–32.
17. Sutton, W. H., Microwave processing of ceramic materials. *Bull. Am. Ceram. Soc.*, **68**(2) (1989) 376–86.
18. Warrier, K. G. K., Varma, H. K., Mani, T. V. & Damodaran, A. D., Rapid method for the preparation of 123 superconductor using microwaves. *J. Am. Ceram. Soc.*, **75**(7) (1992) 1990–2.
19. Janney, M. A., Calhoun, C. L. & Kimrey, H. D., Microwave sintering of solid oxide fuel cell materials: I. Zirconia–8 mol% Yttria. *J. Am. Ceram. Soc.*, **75**(2) (1992) 341–6.
20. Aliouat, M., Mazo, L. & Desgardin, G., Microwave sintering of oxides. *Mater. Res. Soc. Symp. Proc.*, **189** (1990) 229–35.
21. Selmi, F., Guerin, F., Yu, X. D., Varadan, V. K. Varadan, V. V. & Komarneni, S., Microwave calcination and sintering of barium strontium titanate. *Mater. Lett.*, **12** (1992) 424–8.
22. Al-Allak, H. M., Parry, T. V., Russell, G. J. & Woods, J., Effects of aluminum on the electrical and mechanical properties of PTCR $BaTiO_3$ ceramics as a function of the sintering temperature. *J. Mater. Sci.*, **23** (1988) 1083–9.
23. German, R. M., Sintering. In *Powder Metallurgy Science,* Metal Powder Industries Federation, Princeton, New Jersey, 1984, pp. 145–200.
24. Amin, A. & Holmes, M. B., Pressure and temperature dependencies of the direct-current resistance of semiconducting (Ba, Sr)TiO_3 and $(B_a, P_d)TiO_3$. *J. Am, Ceram. Soc.* **71**(12) (1988) C482–3.
25. Herbert, J. M., Positive temperature coefficient (PTC) resistors. In *Ferroelectric Transducers and Sensors,* Gordon and Breach Science Publishers Ltd., London, 1982, pp. 157.